Angewandte Chemie International Edition

DOI: 10.1002/anie.201302315

Surface Chemistry

Chemical Activity of Thin Oxide Layers: Strong Interactions with the Support Yield a New Thin-Film Phase of ZnO

*Vadim Schott, Harald Oberhofer, Alexander Birkner, Mingchun Xu, Yuemin Wang, Martin Muhler, Karsten Reuter, and Christof Wöll**

Small Cu particles supported on and most likely activated by a ZnO substrate are the active component in the industrial catalyst used to convert syngas (H_2, CO, CO_2) into methanol, the third most important chemical product worldwide. Although a topic of intense research, the nature of the active site is still under debate.[1] Recently, it has been pointed out that Zn^0 atoms present at the surfaces of the Cu particles exhibit pronounced chemical activity and could explain some of the experimental findings.[2] Another interesting suggestion is the presence of a thin layer of ZnO_x species which forms on the surface of the Cu particles under reaction conditions.[3,4] The importance of such thin oxide layers on the surface of metals under reaction conditions has already been pointed out in other contexts, where it was found that their chemical properties may differ substantially from those of the corresponding bulk oxides.[5] In the case of ZnO this question is particularly interesting, since strong interactions between ZnO and the supporting metal have been reported for ZnO/Cu[6] and in recent work thin layers of ZnO have been shown to adopt a depolarized, graphitic structure,[7–9] $ZnO_{(gr)}$, different from the wurtzite-type bulk.

The properties of oxide thin films supported on metal substrates have been successfully studied in a number of cases, for example, for thin aluminum oxide films grown by oxidation of Ni/Al alloys.[10,11] In contrast, the chemical activity of ZnO thin films supported on Cu single crystals has been investigated in a few cases only.[12–16] Maroie et al. have investigated the adsorption and oxidation processes for single-crystal brass(110), brass(100), and brass(111) surfaces by X-ray photoelectron spectroscopy (XPS).[17] Brass(110) and brass(111) show the same behavior with regard to the interaction with oxygen: the dissociative adsorption of oxygen on the surface is followed by the growth of thin ZnO layers. Wiame et al. reported that after oxidation of (111)-oriented $Cu_{0.7}Zn_{0.3}$ samples at room temperature the surface is covered by ZnO islands; it was suggested that these islands have (0001) and $(000\bar{1})$ surface terminations.[17] A more detailed characterization of the chemical properties of the thin ZnO layers was not carried out in this early work.

In the present paper we report a detailed multitechnique investigation of a brass(111) single-crystal substrate (Cu/Zn ratio 9:1) subjected to different oxidation procedures using scanning tunneling microscopy (STM), X-ray photoelectron spectroscopy (XPS), and Fourier transform infrared spectroscopy (FTIR) under ultrahigh vacuum (UHV) conditions. The experimental findings are then interpreted by comparison with the results of a rather extensive set of density functional theory (DFT) calculations. Our results reveal the growth of thin ZnO adlayers with chemical properties that are markedly different from those of normal, wurtzite-type ZnO substrates.

XPS data recorded for the brass(111) surface before and after different oxidation procedures for two different exit angles of the photoelectrons are shown in Figure 1. Since it is difficult to discriminate between Cu and Cu^+ on the basis of XPS data, also the corresponding results from Auger electron spectroscopy (AES) are shown. For the clean brass(111) substrate the data indicate a Zn atom concentration of 5%, clearly lower than the 10% expected based on the bulk Cu/Zn ratio. Upon oxidation, the XPS data reveal an increase of the surface Zn concentration. Since it is a crucial question whether, in addition to Zn^{2+}, also Cu^+ or Cu^{2+} is present, we have carefully analyzed the XPS and AES data. Neither in the Cu 2p XPS data nor in the Cu $L_3M_{45}M_{45}$ Auger data were the characteristic signatures of Cu^+ or Cu^{2+} species resulting from an oxidation of copper atoms detected. Cu^+ exhibits a $L_3M_{45}M_{45}$ peak at electron kinetic energies of 915 eV–917 eV,[25] which is clearly absent in the present data (see Figure 1). This observation, which agrees with the conclusions presented in a previous study by Rameshan et al.,[18] is expected, since in the presence of the less noble Zn one would expect the formation of ZnO to precede that of Cu_xO. Oxidation at elevated temperatures results in a substantial increase of the Zn^{2+} signal, revealing the formation of thicker ZnO adlayers. The thickness of these thin ZnO layers was determined from the intensity of the Zn $2p_{3/2}$ and Cu $2p_{3/2}$ XPS signals. Exposure of the samples to 500 L of O_2 at room temperature yields a ZnO adlayer with an average thickness of about 1.7 Å, consistent with the presence of a monolayer. More extended exposures to oxygen at room temperature did not result in a significant further increase of the thickness of the ZnO layer. Even the oxidation of the brass substrate at

---

[*] Dr. V. Schott, Dr. A. Birkner, Dr. M. Xu, Dr. Y. Wang
Chair of Physical Chemistry
Ruhr-University Bochum (Germany)
Dr. H. Oberhofer, Prof. Dr. K. Reuter
Chair of Theoretical Chemistry
Technical University of Munich (Germany)
Dr. Y. Wang, Prof. Dr. M. Muhler
Laboratory of Technical Chemistry
Ruhr-University Bochum (Germany)
Prof. Dr. C. Wöll
Institute of Functional Interfaces (IFG)
Karlsruhe Institute of Technology (KIT)
Karlsruhe (Germany)
E-mail: Christof.Woell@kit.edu

Supporting information for this article is available on the WWW under http://dx.doi.org/10.1002/anie.201302315.

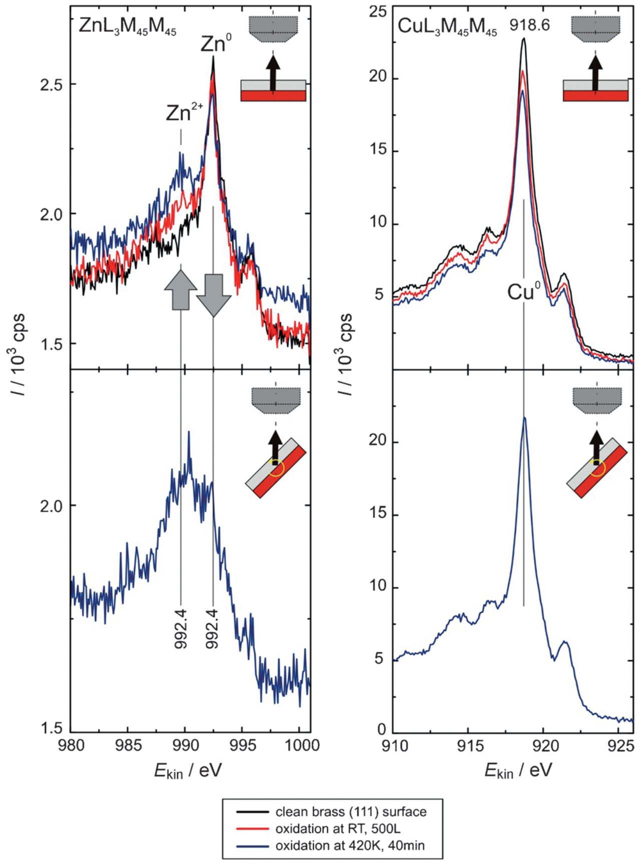

Figure 1. Top: $ZnL_3M_{45}M_{45}$ and $CuL_3M_{45}M_{45}$ Auger spectra before (black curve) and after oxidation at room temperature (red curve) and 420 K (blue curve) recorded at the normal photoelectron exit angle. Bottom: Auger spectra recorded at a grazing exit angle for a sample oxidized at 420 K. cps = counts per second.

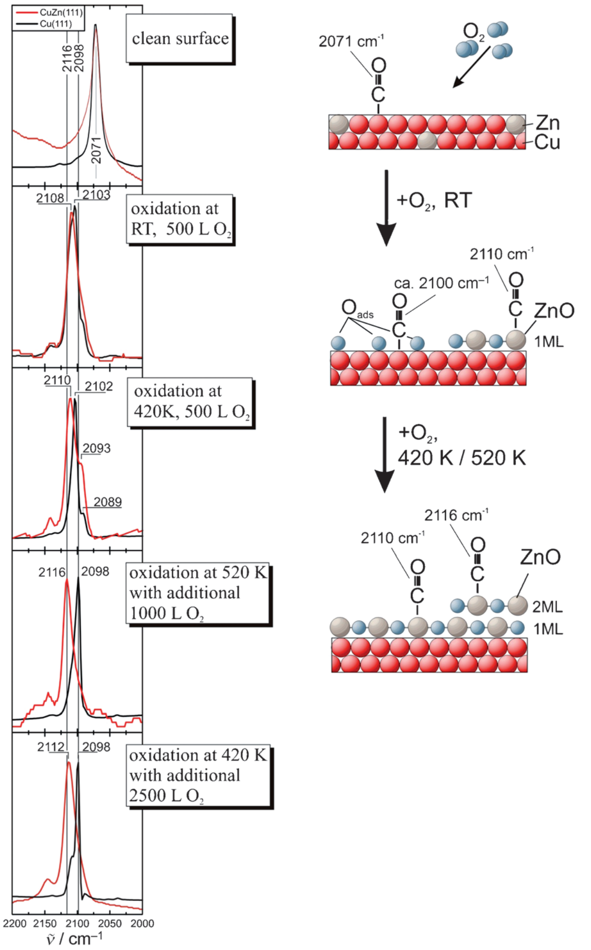

Figure 2. Left: Comparison of RAIRS results for the adsorption of CO on brass(111) and Cu(111) surfaces (normalized representation of spectra). Right: Model of CO adsorption on the brass(111) surface. The corresponding values for the CO stretch frequency are indicated.

higher temperatures (520 K) resulted in a slight, 20% increase in thickness only.

STM data recorded for these ZnO adlayers were consistent with the presence of thin ZnO layers with a thickness of one to two monolayers (ML) (see Figure S2 in the Supporting Information). The resolution of the STM micrographs, however, was not sufficient to resolve the internal structure of the ZnO islands. LEED (low-energy electron diffraction) experiments did not show the formation of an ordered adlayer, in agreement with the STM data.

A rather surprising observation was made when the chemical activity of the ZnO adlayers formed by oxidation of the brass substrate was determined by exposure to CO. The CO stretch frequency measured using grazing incidence reflection absorption IR spectroscopy (RAIRS) displayed an anomalous red-shift by about 50 cm^{-1} relative to the normal stretch for CO adsorbed on ZnO. We continue the discussion by considering first the data for the thickest ZnO adlayer (2 ML) prepared by oxidation at 520 K (see Figure 2 bottom). The IR data reveal a fairly sharp CO band at an unusually low frequency of 2116 cm^{-1}. This value does not agree with any of the CO stretch frequencies reported previously for CO adsorbed on ZnO substrates. A red-shift of around 70 cm^{-1} is evident relative to previous single-crystal data (2192 cm^{-1} for ZnO(10$\bar{1}$0),[26] 2178 cm^{-1} for the Zn-terminated ZnO(0001)[27]) as well as for CO adsorbed on ZnO powders (2187 cm^{-1}).[28] The anomalous band at 2116 cm^{-1} cannot be due to CO bound to Cu or oxidized Cu atoms, as evidenced by careful experiments for CO adsorbed on an oxidized Cu(111) surface (see Figure 2 and Figure S3).

In line with the red-shift of the CO stretch frequency measured for the thin, brass-supported ZnO layer relative to normal wurtzite ZnO, we observed an increase of the CO binding energy. IR spectra recorded at increasing temperature showed that desorption of CO takes place at about 200 K (see Figure S4 in the Supporting Information), corresponding to a binding energy of about 0.54 eV. This value is substantially higher than that reported previously for CO adsorbed on single-crystal wurtzite reference surfaces: 0.32 eV for ZnO(10$\bar{1}$0), 0.28 eV for Zn-ZnO(0001), and 0.18 eV for O-ZnO(000$\bar{1}$).[29]

The results for thinner ZnO layers prepared by oxidation of the surface at room temperature with a thickness of 0.19 nm (corresponding to one monolayer) are fully consistent with these results, the main difference being that the CO band was found to be slightly (6 cm^{-1}) red-shifted (2108 cm^{-1}–2110 cm^{-1}, see Figure 2 and Figure S4).

Note that the IR experiments demonstrate that the oxide film is completely closed. Any bare parts of the brass substrate would show the typical CO stretch frequency of 2071 cm^{-1} (see Figure 2). The presence of a closed oxide film is consistent with the STM data and also excludes the presence of a substantial amount of Cu/ZnO interface sites (see Figure S6), which have been discussed in previous work.[2] When nonclosed ZnO films (see Figure S6 in the Supporting Information) were prepared intentionally by exposure to small amounts of O_2 (see Figure S5), such Cu/ZnO interface sites were found to give rise to a CO band located at 2091 cm^{-1}. This band, however, was found to be absent in samples exposed to more O_2 which yielded closed ZnO films.

In previous work also the interaction of pyridine has been shown to be rather sensitive to the chemical nature of ZnO surfaces.[30] Whereas pyridine was found to adsorb at room temperature on the Zn-terminated polar surface of ZnO and ZnO(0001), and on the mixed terminated ZnO $(10\bar{1}0)$ surface, for the oxygen-terminated surface, ZnO$(000\bar{1})$ no binding at room temperature is observed.[30] In the present case, pyridine did not adsorb on the thin, brass-supported ZnO adlayers at room temperature. XPS indicated that only after the substrate had been cooled down to temperatures below 120 K was the formation of a pyridine adlayer observed. This experimental result is in apparent contradiction to the CO adsorption experiments: whereas for CO the binding energy to the thin ZnO adlayers is found to increase relative to the wurtzite surfaces, pyridine binds substantially more weakly.

The experiments presented above clearly demonstrate that the oxide formed on the surface of our brass substrates cannot correspond to "normal" (wurtzite) ZnO. In a number of previous studies it has been proposed that thin layers of ZnO exposing a polar surface, (0001) or $(000\bar{1})$, adopt a structure which is different from the normal wurtzite structure. This new structure referred to as graphitic ZnO or $ZnO_{(gr)}$ consists of ZnO(0001) planes which adopt an almost planar structure. This graphitic structure was first proposed on theoretical grounds[7] and was later confirmed on the basis of experimental findings.[8,9] In these structures the Zn^{2+} ions are not fourfold but only threefold coordinated. The formal charge state, however, still corresponds to Zn^{2+}. An important consequence of the presence of essentially planar, depolarized ZnO(0001) sheets is that the electrostatic instability of the ZnO(0001) wurtzite polar surfaces is removed.[7]

In order to test whether the different chemical properties observed here can be explained by the presence of such thin layers of $ZnO_{(gr)}$ and to resolve the apparent contradiction referred to above (high binding energy for CO, low binding energy for pyridine) we have carried out an extensive theoretical analysis employing DFT calculations. While we were able to confirm earlier theoretical studies[7] in that $ZnO_{(gr)}$ corresponds to a stable structure for free, unsupported slabs, this modification of zinc oxide was found to be unstable whenever brought into contact with a Cu substrate. For a number of different choices for the unit cell size and film/slab registry, geometry optimization always resulted in pronounced aplanar distortions of the planar $ZnO_{(gr)}$ layers. In the optimized geometry displayed in Figure 3 the structure is halfway between the graphitic and the wurtzite modifications, with layers that are substantially compressed relative to the wurtzite modification (distance between Zn and O plane on average 0.19 A, compared to 0.39 A for wurtzite) but are clearly not planar as in $ZnO_{(gr)}$. We attribute these aplanar distortions, which are absent for $ZnO_{(gr)}$ films on Ag(111)[8] and Pd(111),[9] to the pronounced mismatch of the lattice constants of the ZnO adlayer and the Cu(111) substrate, as well as to the reactivity of Cu(111) favoring an sp^3-type hybridization within the ZnO overlayer.

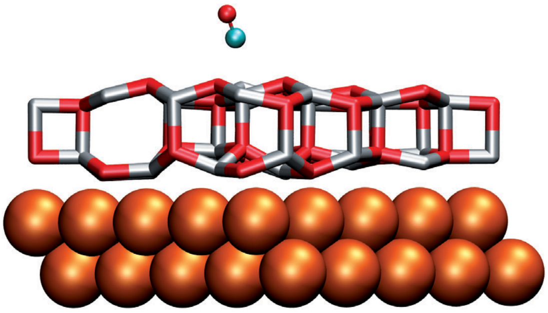

Figure 3. Theoretical results for the structure of a ZnO bilayer supported on a Cu(111) substrate; CO binds through its carbon atom to the top Zn cations. This new thin-film phase differs from wurtzite in both geometry and chemical activity.

A theoretical analysis of the geometry-optimized two-layer ZnO slab on the Cu(111) substrate furthermore demonstrates that the distortion of the wurtzite lattice is accompanied by a substantial charge flow. The Mulliken charge on the Zn ions amounts to +0.74, compared to +0.94 for the ZnO$(10\bar{1}0)$ surface. Of course, this increased electron density at the Zn cations changes their chemical properties and leads to a reduction in Lewis acidity, qualitatively explaining the reduced binding energy for pyridine, a weak Lewis base. At the same time, one would expect the higher Zn electron density to increase the back-donation into the $2\pi^*$ orbital of adsorbed CO, thus causing a red-shift of the CO stretch frequency and an increase of the CO–substrate binding energy, in accord with the experimental observation. Note that such $Zn^{\delta+}$ species have been proposed in a number of previous works (in the context of interfacial Cu/ZnO sites[2] or ZnO_x species[3,4]).

In order to put these heuristic arguments on a solid quantitative basis, we have carried out an explicit calculation of the adsorbate binding energies and vibrational properties at the distorted ZnO adlayer. Indeed, we find an increased CO binding energy of 520 meV, increased by 160 meV relative to ZnO$(10\bar{1}0)$, in line with the experimental observation. This increase in binding energy, a result of the larger back-bonding to the CO molecule, is accompanied by a pronounced red-shift of the CO stretch frequency. The theoretical value for the red-shift relative to ZnO$(10\bar{1}0)$, 101 cm^{-1}, is again in reasonable agreement with the experimental value of 75 cm^{-1}. Independent support for the hypothesis of a distorted wurtzite ZnO adlayer, henceforth termed $ZnO_{(a)}$, comes from an investigation of the interaction with pyridine, a weak Lewis base. Again using the mixed-terminated $ZnO(10\bar{1}0)$ surface as a reference system we find that the binding energy of pyridine on the distorted $ZnO_{(a)}$ layer, 848 meV, is substantially smaller (by 518 meV) than on $ZnO(10\bar{1}0)$, in perfect agreement with the experimental situation. In the experimental findings the ZnO adlayer formed during oxidation was found to be disordered. Since the CO titration experiments demonstrate that the oxide film is fully closed, we feel that the conclusions drawn from the theoretical calculations for a periodic overlayer carried out for a distorted ZnO film are nevertheless fully valid.

Altogether, the experimental findings and the theoretical results allow us to propose a rather concise explanation for the unexpected chemical properties of the thin ZnO adlayers formed on the brass surface: Due to the interaction with the underlying substrate these layers adopt a distorted structure in between the ideal wurtzite(0001) and the planar modification of ZnO, $ZnO_{(gr)}$. This behavior somewhat similar to that reported for the rumpling of FeO monolayers on Pt(111).[31] In the new, distorted structure reported here for ZnO, $ZnO_{(a)}$, the lower oxidation state of the Zn cations leads to a pronounced change of the chemical properties, as evidenced by the interaction with CO and pyridine. The increased electron density at the Zn cations increases the CO binding energy through increased back-bonding but at the same time it decreases the binding energy to pyridine because the affinity to the lone pair of the pyridine N atom is reduced by the presence of the additional charge.

In the industrial catalyst Cu nanoparticles are in close contact with ZnO nanoparticles of roughly the same size, between 5 to 15 nm.[12] Thus, one may speculate that under the strongly reducing steady-state conditions, partial reduction of ZnO particles through strong metal–support interaction (SMSI) adjusts the oxidation state of Zn to a less strongly oxidized $Zn^{\delta+}$ state. We propose that the unique role of ZnO in the industrial catalyst is related to the stability of this intermediate oxidation state formed under the reducing potential of methanol synthesis conditions.

Experimental Section

In our study we have used two identical brass(111) single crystals with a composition of 90 % Cu and 10 % Zn (MaTeck). The samples were prepared by cycles of Ar^+ sputtering at room temperature (800 V, 1 μA), followed by annealing at 430 K.

The measurements were carried out using three different UHV chambers. The UHV-STM system (JSPM-4500S, JEOL) consists of a load-lock, a preparation and an analysis chamber. The analysis chamber was equipped with a scanning electron microscope (SEM), STM, and XPS with Mg/Al anodes. It was possible to cool the samples to temperatures of 70 K and to anneal the samples at 1000 K. In the preparation chamber, a sputter gun, LEED optics, and a quadrupole mass spectrometer were situated. The XPS experiments were performed in the second apparatus, a modified Leybold MAX 200 XPS system with Mg/Al anodes, plus a monochromatic X-ray source (Al anode), along with the option for ion scattering spectroscopy (ISS) and low-energy electron diffraction. FTIR experiments were performed in an UHV apparatus, which contained a state-of-the-art vacuum IR spectrometer (Bruker, VERTEX 80v).[19]

All theoretical calculations were performed using the CASTEP[20] plane-wave DFT package, using library ultrasoft pseudo-potentials and an energy cutoff of 380 eV, and treating electronic exchange and correlation with the GGA functional due to Perdew, Burke, and Ernzerhof.[21] K-point sampling was performed on a $5\times5\times1$ regular grid and dispersion forces were treated using the Tkatchenko–Scheffler semiempirical correction scheme.[22] The surface system was represented by supercell geometries. For one- or two-layer-thick $ZnO_{(gr)}$ and ZnO(0001) overlayers we used (4×4) Cu(111) surface unit cells, and treated the films either free-standing, asymmetrically adsorbed on one side of a two-layer Cu(111) slab, or symmetrically adsorbed on both sides of a four-layer Cu(111) slab. For $ZnO(10\bar{1}0)$ we used four-layer slabs and a (2×2) cell. We validated that the residual strain in the interfacial systems does not affect the conclusions drawn below by performing calculations both at the optimized lateral Cu lattice constant (and straining the film) and at the optimized lateral ZnO lattice constant (and straining the slab). For the isolated polar ZnO(0001) wurtzite film the dipole moment of the simulation box was compensated by placing a mirror image of the surface system at a distance of 20 Å. At all films CO was found to bind preferably atop Zn atoms. Harmonic CO stretch frequencies were then computed with a finite difference scheme, yielding a gas-phase value of 2181 cm^{-1} in close agreement to earlier calculations.[23] Compensating the known offset to the experimental value (2143 cm^{-1} [24]), all frequency shifts for adsorbed CO are given relative to the gas-phase value.

Received: March 19, 2013
Revised: June 19, 2013

Keywords: catalyst–support interactions · copper · heterogeneous catalysis · surface chemistry · zinc oxide

[1] J. B. Hansen, P. E. H. Nielsen, *Handbook of Heterogeneous Catalysis* (Eds.: G. Ertl, H. Knözinger, F. Schüth, J. Weitkamp), Wiley-VCH, Weinheim, **2008**, pp. 2920–2949.
[2] M. Behrens, F. Studt, I. Kasatkin, S. Kuhl, M. Havecker, F. Abild-Pedersen, S. Zander, F. Girgsdies, P. Kurr, B. L. Kniep, M. Tovar, R. W. Fischer, J. K. Norskov, R. Schlogl, *Science* **2012**, *336*, 893–897.
[3] R. Naumann d'Alnoncourt, M. Kurtz, H. Wilmer, E. Loffler, V. Hagen, J. Y. Shen, M. Muhler, *J. Catal.* **2003**, *220*, 249–253.
[4] R. Naumann d'Alnoncourt, X. Xia, J. Strunk, E. Loffler, O. Hinrichsen, M. Muhler, *Phys. Chem. Chem. Phys.* **2006**, *8*, 1525–1538.
[5] S. Shaikhutdinov, H.-J. Freund, *Annu. Rev. Phys. Chem.* **2012**, *63*, 619–633; Y. Martynova, B.-H. Liu, M. E. McBriarty, I. M. N. Groot, M. J. Bedzyk, S. Shaikhutdinov, H.-J. Freund, *J. Catal.* **2013**, *301*, 227–232.
[6] J.-D. Grunwaldt, A. M. Molenbroek, N.-Y. Topsøe, H. Topsøe, B. S. Clausen, *J. Catal.* **2000**, *194*, 452.
[7] F. Claeyssens, C. L. Freeman, N. L. Allan, Y. Sun, M. N. R. Ashfold, J. H. Harding, *J. Mater. Chem.* **2005**, *15*, 139–148; C. L. Freeman, F. Claeyssens, N. L. Allan, J. H. Harding, *Phys. Rev. Lett.* **2006**, *96*, 066102.
[8] C. Tusche, H. L. Meyerheim, J. Kirschner, *Phys. Rev. Lett.* **2007**, *99*, 026102.
[9] G. Weirum, G. Barcaro, A. Fortunelli, F. Weber, R. Schennach, S. Surnev, F. P. Netzer, *J. Phys. Chem. C* **2010**, *114*, 15432–15439.
[10] R. M. Jaeger, H. Kuhlenbeck, H. J. Freund, M. Wuttig, W. Hoffmann, R. Franchy, H. Ibach, *Surf. Sci.* **1991**, *259*, 235–252.
[11] S. Ulrich, N. Nilius, H. J. Freund, *Surf. Sci.* **2007**, *601*, 4603–4607.
[12] M. Sano, T. Adaniya, T. Fujitani, J. Nakamura, *Surf. Sci.* **2002**, *514*, 261–266.

[13] E. V. Thomsen, M. Christiansen, J. Onsgaard, *Appl. Surf. Sci.* **1992**, *62*, 189 – 194.
[14] S. S. Fu, G. A. Somorjai, *Surf. Sci.* **1990**, *237*, 87 – 98.
[15] S. S. Fu, G. A. Somorjai, *Appl. Surf. Sci.* **1991**, *48 – 49*, 93 – 103.
[16] S. S. Fu, G. A. Somorjai, *Langmuir* **1992**, *8*, 518 – 524.
[17] S. Maroie, P. A. Thiry, R. Caudano, J. J. Verbist, *Surf. Sci.* **1983**, *127*, 200 – 222; F. Wiame, V. Maurice, P. Marcus, *Surf. Sci.* **2007**, *601*, 4402 – 4406.
[18] C. Rameshan, W. Stadlmayr, S. Penner, H. Lorenz, N. Memmel, M. Hävecker, R. Blume, D. Teschner, T. Rocha, D. Zemlyanov, A. Knop-Gericke, R. Schlögl, B. Klötzer, *Angew. Chem.* **2012**, *124*, 3057; *Angew. Chem. Int. Ed.* **2012**, *51*, 3002.
[19] Y. Wang, A. Glenz, M. Muhler, C. Wöll, *Rev. Sci. Instrum.* **2009**, *80*, 113108.
[20] S. J. Clark, M. D. Segall, C. J. Pickard, P. J. Hasnip, M. J. Probert, K. Refson, M. C. Payne, *Z. Kristallogr.* **2005**, *220*, 567 – 570.
[21] J. P. Perdew, K. Burke, M. Ernzerhof, *Phys. Rev. Lett.* **1996**, *77*, 3865 – 3868.
[22] A. Tkatchenko, M. Scheffler, *Phys. Rev. Lett.* **2009**, *102*, 073005.
[23] Y. Wang, S. de Gironcoli, N. S. Hush, J. R. Reimers, *J. Am. Chem. Soc.* **2007**, *129*, 10402 – 10407.
[24] “Constants of Diatomic Molecules”: K. P. Huber, G. Herzberg, *Molecular Spectra and Molecular Structure*, *Vol. 4*, New York, Van Nostrand Reinhold, **1979**.
[25] S. Schimpf, A. Rittermeier, X. N. Zhang, Z. A. Li, M. Spasova, M. W. E. van den Berg, M. Farle, Y. M. Wang, R. A. Fischer, M. Muhler, *ChemCatChem* **2010**, *2*, 214 – 222.
[26] Y. M. Wang, X. Y. Xia, A. Urban, H. S. Qiu, J. Strunk, B. Meyer, M. Muhler, C. Wöll, *Angew. Chem.* **2007**, *119*, 7456 – 7459; *Angew. Chem. Int. Ed.* **2007**, *46*, 7315 – 7318.
[27] L. Jin, Y. Wang, **2013**, unpublished results.
[28] H. Noei, C. Wöll, M. Muhler, Y. M. Wang, *Appl. Catal. A* **2011**, *391*, 31 – 35.
[29] C. Wöll, *Prog. Surf. Sci.* **2007**, *82*, 55 – 120.
[30] S. Hövel, C. Kolczewski, M. Wühn, J. Albers, K. Weiss, V. Staemmler, C. Wöll, *J. Chem. Phys.* **2000**, *112*, 3909 – 3916.
[31] J. Goniakowski, C. Noguera, *Phys. Rev. B* **2009**, *79*, 155433; C. Noguera, J. Goniakowski, *Chem. Rev.* **2013**, *113*, 4073.